The Journal of Neuroscience, June 1, 1996, 16(11):3775–3789

A Primary Acoustic Startle Pathway: Obligatory Role of Cochlear Root Neurons and the Nucleus Reticularis Pontis Caudalis

Younglim Lee,[1] Dolores E. López,[2] Edward G. Meloni,[1] and Michael Davis[1]

[1]Yale University School of Medicine, Abraham Ribicoff Research Facilities of The Connecticut Mental Health Center, New Haven, Connecticut 06508, and [2]Departamento de Biología Celular y Patología, Facultad de Medicina, Universidad de Salamanca, Salamanca, Spain

Davis et al. (1982) proposed a primary acoustic startle circuit in rats consisting of the auditory nerve, posteroventral cochlear nucleus, an area near the ventrolateral lemniscus (VLL), nucleus reticularis pontis caudalis (PnC), and spinal motoneurons. Using fiber-sparing lesions, the present study reevaluated these and other structures together with the role of neurons embedded in the auditory nerve [cochlear root neurons (CRNs)], recently hypothesized to be involved in acoustic startle. Small electrolytic lesions of the VLL or ventrolateral tegmental nucleus (VLTg) failed to eliminate startle. Large electrolytic lesions including the rostral ventral nucleus of the trapezoid body (rVNTB) and ventrolateral parts of PnC or lesions of the entire PnC blocked startle. However, small NMDA-induced lesions of the rVNTB failed to block startle, making it unlikely that the rVNTB itself is part of the startle pathway. In contrast, NMDA lesions of the full extension of the ventrolateral part of the PnC blocked startle completely, suggesting that the ventrolateral part of the PnC is critically involved. Bilateral kainic acid lesions of CRNs also blocked the startle reflex completely, providing the first direct evidence for an involvement of CRNs in startle. This blockade probably was not caused by damage to the auditory nerve, because the lesioned animals showed intact compound action potentials recorded from the ventral cochlear nucleus. Hence, a primary acoustic startle pathway may involve three synapses onto (1) CRNs, (2) neurons in PnC, and (3) spinal motoneurons.

Key words: startle; cochlear root neurons; reticular formation; cochlear nucleus; compound action potential; lateral lemniscus; ventral tegmentum

The acoustic startle reflex is a short-latency behavior elicited by a sudden and intense acoustic stimulus. The amplitude of the acoustic startle reflex can be modified by various behavioral and pharmacological treatments. In rodents, startle exhibits within as well as between session habituation (Prosser and Hunter, 1936; Landis and Hunt, 1939; Hoffman and Stitt, 1969; Davis, 1970; Groves and Thompson, 1970; Leaton, 1976; Adams and Geyer, 1981; Kokkinidis, 1986; Leaton and Supple, 1986; Swerdlow et al., 1986; Geyer and Braff, 1987; Jordan, 1989; Parham and Willott, 1990), sensitization to environmental stimuli (Groves and Thompson, 1970; Davis, 1974; Cory and Ison, 1979; Russo and Ison, 1979), prepulse facilitation and inhibition (Hoffman et al., 1969; Ison and Hammond, 1971; Hoffman and Ison, 1980; Ison, 1982; Mansbach and Geyer, 1991; Swerdlow et al., 1992; Koch et al., 1993), and enhancement by previous fear conditioning (Brown et al., 1951; Davis and Astrachan, 1978) or shock stress (Korn and Moyer, 1965; Davis, 1989; Krase et al., 1994). Furthermore, the acoustic startle response (cf. Davis, 1980), as well as fear-potentiated startle (cf. Davis et al., 1993) and prepulse inhibition (cf. Swerdlow et al., 1992), is sensitive to a variety of different drugs, making the reflex a useful animal model of sensorimotor reactivity, fear, and attention. Finally, results obtained in rats have consistently proven to generalize to humans (Landis and Hunt, 1939; Davis and Heninger, 1972; Graham, 1975; Braff et al., 1978; Ornitz et al., 1986; Lang et al., 1990; Grillon et al., 1991; Braff et al., 1992; Cook et al., 1992; Bradley et al., 1993; Fillon et al., 1993; Lipp et al., 1994).

Because the acoustic startle reflex has an extraordinarily short latency (e.g., 6–8 msec measured electromyographically in the hindleg muscles) (Ison et al., 1973), it must be mediated by a simple pathway. Using a variety of techniques, our laboratory proposed a primary acoustic startle circuit in rats that consisted of the auditory nerve, posteroventral cochlear nucleus (PVCN), an area ventral and medial to the ventral nucleus of the lateral lemniscus (VLL), the nucleus reticularis pontis caudalis (PnC), and motoneurons in the spinal cord (Davis et al., 1982).

Although lesion and stimulation data generally supported different aspects of this circuitry (Davis et al., 1982; Yeomans et al., 1989; Pellet, 1990; Koch et al., 1992; Yeomans and Cochrane, 1993; Yeomans et al., 1993; Lingenhöhl and Friauf, 1994; Frankland et al., 1995), relatively large lesion sizes and the nonselective nature of electrolytic lesions and electrical stimulation did not allow us to delineate definitely some important details throughout the proposed neural pathway. For example, lesions of the VLL in the original study often included the paralemniscal zone (PL), the ventrolateral tegmental area (VLTg), the rostral part of the ventral nucleus of the trapezoid body (rVNTB, called the rostroperiolivary region by some authors), and the anterior and ventrolateral areas of the PnC. Therefore, the present studies reevaluated the role of structures implicated previously in the primary acoustic startle circuit using discrete bilateral electrolytic and chemical lesion techniques.

Received Nov. 8, 1995; revised March 13, 1996; accepted March 19, 1996.

This research was supported by National Institute of Mental Health Grants MH-25642 and MH-47840, a grant from the Air Force Office of Scientific Research and Research Scientist Development Award MH-00004 to M.D., and by the FIS 94/1403 and DGICYT PB-93 0610-CO2 from the Spanish government.

Correspondence should be addressed to Dr. Michael Davis, Yale University School of Medicine, Abraham Ribicoff Research Facilities of The Connecticut Mental Health Center, 34 Park Street, New Haven, CT 06508.

In addition, we also evaluated the possible role of cochlear root neurons (CRNs) in acoustic startle responses. In several species including rats and humans, a cluster of neurons have been found embedded in the eighth cranial nerve. The CRNs receive input from the cochlea and give off collaterals terminating contralaterally in the ventrolateral part of the PnC (López et al., 1993b). Because it has been suggested that CRNs may be involved in the acoustic startle response (López et al., 1993a,b; Lingenhöhl and Friauf, 1994), we also tested their role in the acoustic startle reflex.

MATERIALS AND METHODS

Animals. The animals were male albino Sprague–Dawley rats (Charles River, Wilmington, MA) that weighed between 330 and 370 gm. Before surgery, the rats were housed in group cages of three and maintained on a 12 hr light/dark cycle (light on at 7:00 A.M.) with food and water continuously available. After surgery, the animals were housed singly.

Startle apparatus. Five separate stabilimeters were used to record the amplitude of the startle responses. Each stabilimeter consisted of an 8 cm × 15 cm × 15 cm Plexiglas and wire mesh cage suspended between compression springs within a steel frame. Cage movement resulted in displacement of an accelerometer where the resultant voltage was proportional to the velocity of cage displacement. The analog output of the accelerometer was amplified and digitized on a scale of 0–4096 units by a MacADIOS II board (GW Instruments, Somerville, MA) interfaced to a Macintosh II microcomputer. Startle amplitude was defined as the peak accelerometer voltage that occurred during the first 200 msec after onset of the startle stimulus. The stabilimeters were housed in a ventilated, sound-attenuating chamber (2.5 m × 2.5 m × 2 m) (Industrial Acoustic).

The startle stimuli were delivered by high-frequency speakers (Radio Shack Supertweeters, range, 5–40 kHz) located 10 cm behind each stabilimeter. High-frequency startle stimuli were 50 msec bursts of white noise, generated by a Lafayette 15011 noise generator (0.02–20 kHz), with a rise–decay time of 5 msec at various intensities (90, 95, 100, 105, or 115 dB). Throughout all experiments, background white noise (0.02–20 kHz) of 55 dB sound pressure level (SPL) was provided by a white noise generator (Grason-Stadler, model 901B) and delivered by a single Jamocar 70 speaker (range, 0.02–20 kHz) located ~70 cm in front of each cage. SPL measurements were made with a Brüel & Kjær (Marlborough, MA) condenser microphone (type 4133) fitted to a Brüel & Kjær model 2235 sound-level meter (A scale; random input).

Matching. One day before surgery, animals were placed in the startle chambers and, after a 5 min acclimation period, presented with 30 startle stimuli, 10 at each of three intensities (either 90, 95, and 105 dB or 100, 105, and 115 dB) in a semirandom order at a 30 sec interstimulus interval. For NMDA-lesion and kainic acid lesion studies, the animals' activity levels also were recorded by measuring the cage movement in the absence of the startle-eliciting noise bursts. These activity samples occurred 15 sec after each startle trial. The animals subsequently were divided into sham or lesion groups, having similar mean startle amplitudes across the 10 stimuli at each intensity.

Electrolytic lesions. Rats were anesthetized with chloral hydrate (400 mg/kg, i.p.) and placed in a Kopf stereotaxic instrument (model 900) with blunt earbars. The skin was retracted, and bilateral holes were drilled in the skull above the structures to be lesioned. An NE-300 electrode (0.25 mm diameter, insulated to within 0.5 mm of the tip) (Rhodes Medical Instruments) was lowered into the brain, and a lesion was made by passing a 0.1 mA DC current (anode in the brain) for 10–20 sec. Bilateral lesions were made in the VLL (n = 20), PL/VLTg (n = 20), and the rVNTB (n = 30). Bilateral lesions were made using the following coordinates relative to bregma and the following times: VLL, −8.4 mm to bregma [anterior–posterior (AP)], ± 2.3 mm lateral to midline [medial–lateral (ML)], 9.3 mm ventral from skull [dorsal–ventral (DV); 10 sec]; PL/VLTg, −8.3 mm AP, ± 1.6 mm ML, 9 mm DV (15 sec); rVNTB, −8.3 mm AP, ± 1.5 mm ML, 10.3 mm DV (20 sec). The procedure for the sham lesion (n = 5 for each location) was identical, except that no current was delivered.

NMDA lesions. NMDA (Sigma, St. Louis, MO) was dissolved in 0.1 M phosphate buffer (PB), pH 7.4. The animals were anesthetized with Nembutal (50 mg/kg, i.p.) and placed in a Kopf stereotaxic instrument (model 900) with blunt earbars. The skin was retracted, a hole was drilled in the skull, and a 1 μl Hamilton syringe (model 7002) filled with NMDA solution (2 mg/100 μl) was lowered into the structure of interest. Five minutes later, 100 or 200 nl of NMDA solution was infused at a rate of 100 nl/2 min. After the infusion, the syringe remained in the brain for 10 min. All infusions were made bilaterally, and the animals were kept warm with a heating lamp throughout the operation. Lesions were placed in the area of the rVNTB/PnC (n = 20) and the ventrolateral part of the PnC (n = 20) using the following coordinates relative to bregma: rVNTB, −8.0 mm AP, ± 1.5 mm ML, 10.3 mm DV; PnC, −9.3 mm AP, ± 1.3 mm ML, 10.3 mm DV. For the control animals (n = 15), an equivalent amount of PBS was infused into the ventrolateral part of the PnC using the procedures described above.

Kainic acid lesions. Because preliminary data showed that NMDA failed to destroy CRNs after local infusion into the auditory nerve, kainic acid was used to destroy these cells. The animals were anesthetized with Nembutal (50 mg/kg, i.p.) and secured in a Kopf model 1430 stereotaxic frame assembly. To minimize bleeding and trauma to the middle ear, we chose to gain access to the CRNs by inserting a glass micropipette through the cerebellum and then out through the skull via the internal acoustic meatus. To do this, it was necessary to use an angled approach to gain access to these neurons and to use the base of the lambdoid suture as a reference point. The electrode carrier (model 1455) of the stereotaxic instrument was adjusted 20° to the right, and the swivel was fixed at level +6 (turn to left) to reach the left CRNs. To reach the right CRNs, the swivel level was changed to −6 (turn to right), without adjusting the angle of the electrode carrier. The coordinates relative to the base of lambda were −0.9 mm AP, ± 4.3 mm ML, and 0.0 mm DV. Kainic acid (Sigma) was dissolved in 0.1 M PB, pH 7.4, at a concentration of 30 mmol (6.4 mg/ml). In 40 animals, bilateral pressure injection of kainic acid into CRNs was made by using a 3-mm-wide glass pipette pulled to a tip diameter of 50 μm, attached to a Hamilton microsyringe (model 7002). After the proper adjustments were made, the pipette attached to the microsyringe was lowered gently into the brain through the inside of the skull and out through the entrance of the internal acoustic meatus into the auditory nerve. A volume of 200 nl of kainic acid solution was infused at a rate of 100 nl/2 min. After infusion, the pipette remained inside the eighth cranial nerve for 10 min. In 15 control animals, an equivalent amount of PBS was infused, using the procedures described above. The animals were kept warm during the operation with a heating lamp.

Startle response test. After 7–10 d of recovery, the animals again were placed in the startle chambers and given a startle test identical to the matching test.

Compound action potential recording. Because the cell bodies of the CRNs are embedded within the auditory nerve fibers, the integrity of auditory function was examined after the kainic acid lesioning of the CRNs. After the startle response test, auditory evoked field potentials (the compound action potentials) were recorded from the ventral cochlear nucleus (VCN) in representative animals that received bilateral kainic acid (n = 3) or sham lesions (n = 3) of the CRNs. The three animals in the bilateral kainic acid lesion group were chosen because they had a total blockade of the acoustic startle reflex. To be sure that the compound action potential methodology would detect damage to the auditory nerve, six other control rats were given unilateral electrolytic lesions of the CRNs. These animals were anesthetized with Nembutal (50 mg/kg, i.p.) and subjected to electrolytic lesioning of the CRNs using the identical angled approach to the CRNs described above. An NE-300 electrode (0.25 mm diameter, insulated to within 0.5 mm of the tip) (Rhodes Medical Instruments) was lowered into the brain, and a lesion was made by passing a 0.1 mA DC current (anode in the brain) for 30 sec. Lesions were made unilaterally.

Ten days after sham, kainic acid, or electrolytic lesioning of the CRNs, all animals were anesthetized with Nembutal (50 mg/kg, i.p.) and placed in a Kopf stereotaxic instrument with blunt, hollow earbars. Two holes were drilled in the skull (AP −10.8 mm and ML ± 3.8 mm), and 30-gauge stainless steel cannulas were lowered bilaterally into the ventral cochlear nucleus to a point 6 mm below the dura. A bundle of four, 25 μm nichrome wires then was lowered stereotaxically through each guide cannula until the compound action potential could be recorded from each cochlear nucleus in response to acoustic stimuli. Dental cement and 0–80 jeweler's screws secured to the top of the skull held the wire bundles in place when the animals were removed from the stereotaxic device to record compound action potentials.

The acoustic stimuli used to produce these potentials were 2 msec white noise pulses or 10 kHz tones produced by a tone generator (Wavetek, model 182A) connected to an electronic switch (Grason-Stadler, model 829E) to provide a 0.5 msec rise–fall time. The auditory stimuli were delivered through a high-frequency speaker (Radio Shack

supertweeter) placed 3 m above the animals so that all of the electrical artifacts occurred ~3 msec before the sound pressure wave actually reached the animal's ear, allowing artifact-free measurement of the compound action potential. The intensity of the acoustic stimuli (70, 80, and 90 dB) was measured at the animal's ear with a sound-level meter (Brüel & Kjær, model 2235, A scale) presented over an ambient noise level of 45 dB from a white noise generator. The compound action potential was passed through a Fintronics single-unit amplifier (gain 4000×), filtered (0.4–6 kHz), and fed in parallel to an oscilloscope and through an analog-to-digital converter to an IBM AT computer. The compound action potential was recorded and analyzed using an Enhanced Graphics Acquisition and Analysis program (R. C. Electronics, Computerscope).

Biotinylated dextran amine (BDA) injections in the CRNs. To visualize the trajectory and termination of CRNs, an anterograde tracer, BDA, was infused into the CRNs. Using the angled approach described above, unilateral injections of a 10% solution of BDA (Molecular Probes, Eugene, OR) in saline were iontophoretically made into the CRNs by passing pulses of positive current (3–5 μA DC, duty cycle 7 sec) for 15 min. The micropipette was left in place for 15 min after finishing the injection to minimize the leakage of BDA along the electrode track. After a 1 week survival, the animals were anesthetized deeply and perfused intracardially with a mixture of aldehydes (paraformaldehyde 1%, glutaraldehyde 1.25% in PB 0.1 M, pH 7.4). After a cryoprotection in 30% sucrose in PB, 0.1 M, pH 7.4, frozen sections of the brainstem (40 μm thick) were processed to visualize the tracer by standard ABC methods. In short, the sections were rinsed in PB and incubated in Vectastain ABC reagent (1:225) for 90 min. Tissue-band peroxidase was visualized by incubating the sections with 0.07% 3,3′diaminobenzidine and 0.003% hydrogen peroxide in Tris buffer (0.1 M, pH 7.6) for 10–15 min. Finally, the sections were dehydrated gradually using a series of ethanol solutions in increasing concentrations and mounted for light microscopic examination. Alternate 40 μm sections were counterstained with cresyl violet.

Histology: electrolytic lesion and NMDA lesion studies. All animals were killed by chloral hydrate overdose and perfused intracardially with 0.9% saline followed by 10% formalin. The brains then were removed and stored in 10% formalin containing 30% sucrose for at least 3 d. Subsequently, 40 μm frozen coronal sections were cut through the areas containing the lesions, and every third section was mounted on gelatin-coated slides. For verification of the electrolytic lesions, the brain sections were stained with cresyl violet. For NMDA lesion verification, the brain sections were stained using the Klüver–Barrera method (Klüver and Barrera, 1953) to assess damage to cell bodies versus fibers of passage separately.

Histology: kainic acid lesion and CRN-projection studies. Because CRNs are stained very clearly with Calbindin, we used Calbindin immunohistochemical stain for histological verification of CRNs lesions. The animals were killed by chloral hydrate overdose and perfused intracardially with 100 ml of 0.1 M PB, pH 7.4, containing 0.5% of sodium nitrite (Sigma) followed by 1 l of 0.1 M PB, pH 7.4, fixative solution containing 4% paraformaldehyde (Fisher Scientific, Orangeburg, NY), 0.12% glutaraldehyde (Fisher Scientific), and 15% saturated solution of picric acid (Sigma). This extensive perfusion procedure was necessary to remove the brains without damaging the eighth nerve and to enhance the tissue reactivity for the immunohistochemical procedure. Subsequently, 40 μm frozen coronal sections were cut through the brainstem, and every third section was mounted on gelatin-coated slides and prepared for Calbindin staining.

The sections were washed in several changes of PBS and incubated free-floating for 36 hr at 4°C in the primary monoclonal antibody 1/200 (Sigma, ref. C8666) in PBS containing 10% fetal calf serum and 0.3% Triton X-100 0.1 M. The sections were washed in PBS and incubated by gentle shaking with biotinylated anti-mouse immunogammaglobulin (Vector Laboratories, Burlingame, CA, ref. PK 4002) and diluted 1:200 (in PBS containing 10% fetal calf serum and 0.3% Triton X-100 0.1 M) for 2 hr at room temperature. After being rinsed in PBS, the sections were processed by standard ABC method (see previous section). Finally, the sections were dehydrated in a series of ethanol solutions in increasing concentrations and mounted with Entellán using coverslips. To minimize the background endogenous peroxidase reaction before the ABC incubation, the sections were maintained for 10 min in a mixture of buffer, methanol, and commercial (30%) hydrogen peroxide in a ratio of 8:1:1.

RESULTS

Electrolytic lesions

Four VLL, 2 PL/VLTg, and 12 rVNTB animals were excluded after histology because of misplaced lesions, leaving successful electrolytic lesions in 16 VLL, 18 PL/VLTg, and 18 rVNTB animals. Because of their anatomical proximity, lesions of the rVNTB always encroached on some part, if not all, of the area just ventral to the posterior aspect of the ventrolateral part of the nucleus reticularis pontis oralis (PnO). Eight of the 18 lesioned animals retained for analysis had rVNTB lesions combined with lesions of the posterior aspect of the ventrolateral part of the PnO, whereas 10 animals from the intended rVNTB lesion group showed complete lesions of the posterior aspect of the ventrolateral part of the PnO as well as the ventrolateral part of the PnC without damaging the rVNTB area. Therefore, data from these two subgroups of animals were analyzed separately. Histological reconstructions of the smallest and largest electrolytic lesions of the VLL, the PL/VLTg, the rVNTB plus the posterior aspect of the ventrolateral part of the PnO, and the posterior aspect of the ventrolateral part of the PnO plus the ventrolateral part of the PnC are presented with their behavioral data in Figures 1 and 2.

The left panels of Figure 1, *A* and *B*, show that electrolytic lesions of either the VLL or the PL/VLTg did not reduce the amplitude of the startle reflex elicited by the three different noise burst intensities (90, 95, and 105 dB). The right panels of Figure 1, *A* and *B*, show histological reconstructions of the largest and smallest lesions of the VLL and PL/VLTg, respectively. Sham electrolytic lesions of the VLL and the PL/VLTg failed to reduce startle amplitudes, so the data were combined and presented in Figure 1*C*.

The left panel of Figure 2*A* shows that lesions of the rVNTB plus the posterior aspect of the ventrolateral part of the PnO significantly reduced startle amplitude elicited by either 90 dB ($t_{(7)} = 2.95, p < 0.022$), 95 dB ($t_{(7)} = 5.00, p < 0.002$), or 105-dB ($t_{(7)} = 6.93, p < 0.000$) white noise bursts. However, there was still a significant amount of startle in these animals, especially at the 105 dB test intensity. The right panel of Figure 2*A* shows histological reconstructions of the largest and smallest lesions of the rVNTB plus the posterior aspect of the ventrolateral part of the PnO. On the other hand, the left panel of Figure 2*B* shows that electrolytic lesions of the posterior aspect of the ventrolateral part of the PnO plus the ventrolateral part of the PnC resulted in a total blockade of startle at each the three test intensities (90 dB, $t_{(9)} = 6.80, p < 0.000$; 95 dB, $t_{(9)} = 7.94, p < 0.000$; 105 dB, $t_{(9)} = 10.23, p < 0.000$). The right panel of Figure 2*B* shows histological reconstructions of the largest and smallest lesions of the posterior aspect of the ventrolateral part of the PnO plus the ventrolateral part of the PnC. Sham electrolytic lesions of these various areas did not reduce startle amplitudes, so the data were combined and are shown in Figure 2*C*.

NMDA lesions

Of the 40 original rats with NMDA-induced lesions of the rVNTB and PnC, 21 were excluded because of misplaced lesions and/or mostly unilateral damage. Of the 19 remaining animals, 5 were judged to have extensive cell loss in the rVNTB and minor cell loss in the posterior aspect of the ventrolateral part of the PnO; 6 to have extensive cell loss in both the rVNTB and the posterior aspect of the ventrolateral part of the PnO and partial cell loss in the anterior aspects of the ventrolateral part of the PnC, and 8 to have extensive cell loss in both the posterior aspect of the ventrolateral part of the PnO and the anterior and posterior aspects

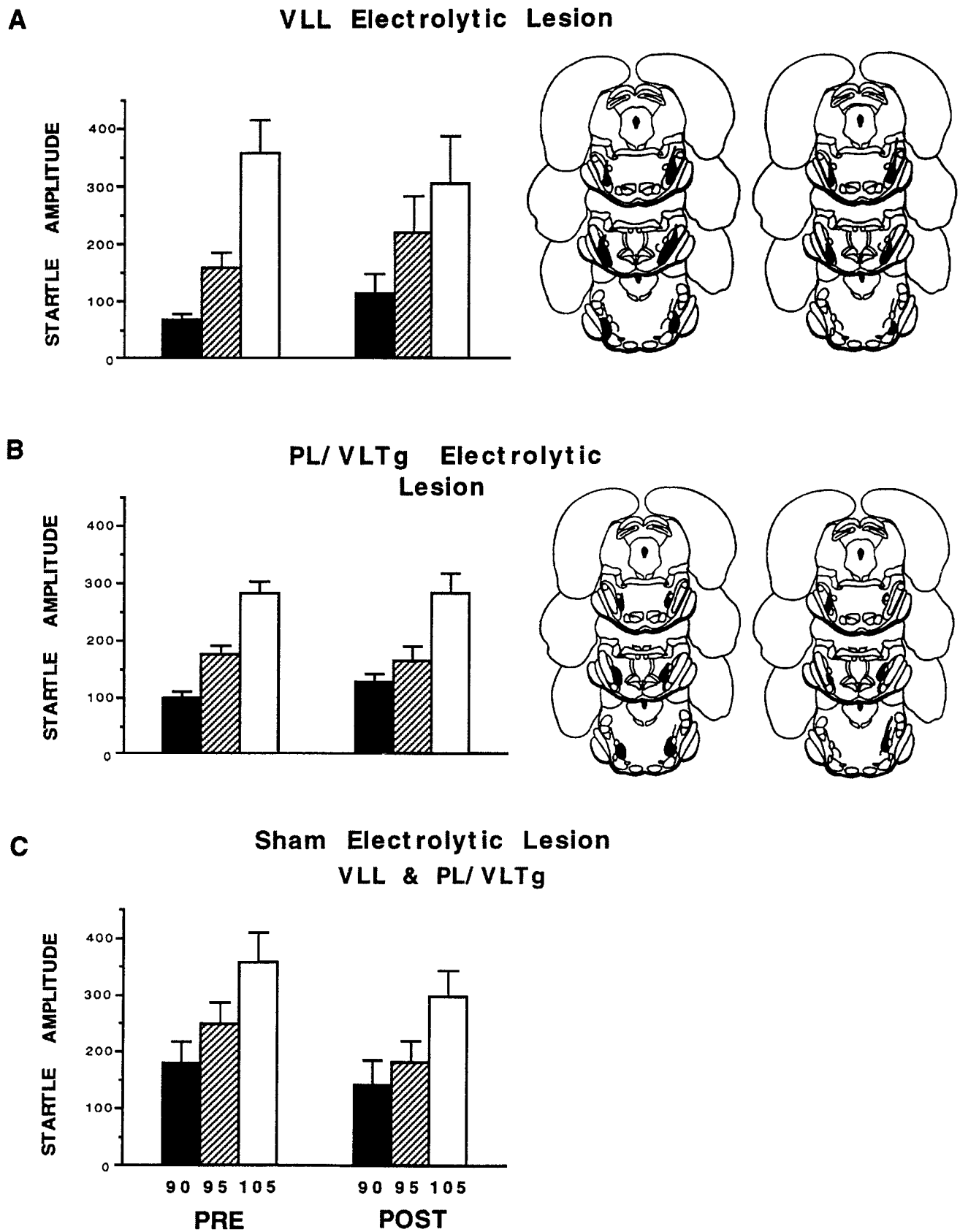

Figure 1. Mean startle amplitude elicited by three different noise burst intensities before and after electrolytic lesioning of the VLL (*A*), or the VLTg (*B*), or sham lesioning of these areas (*C*). Histological reconstructions, based on the atlas of Paxinos and Watson (1986), of the smallest (*left*) and the largest (*right*) electrolytic lesions aimed at the VLL and the PL/VLTg are shown next to the behavioral data. Three plates (bregma −7.80, −8.00, and −8.30 mm) used in histological reconstructions of lesions were taken from Paxinos and Watson (1986).

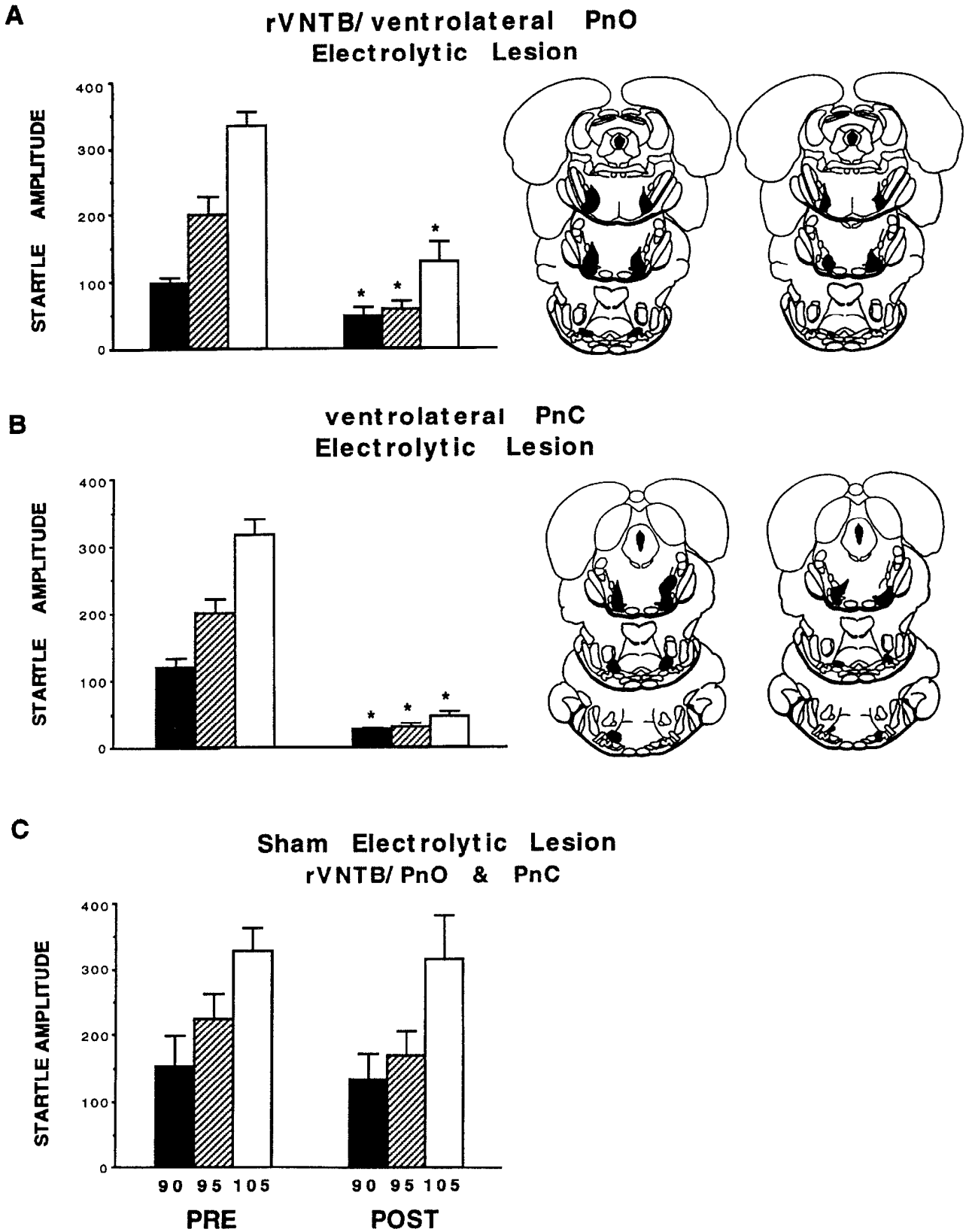

Figure 2. Mean startle amplitude elicited by three different noise burst intensities before and after electrolytic lesioning of the rVNTB combined with the ventrolateral part of the PnO (*A*), the ventrolateral part of the PnC alone (*B*), or sham electrolytic lesioning of the rVNTB or the PnC (*C*). *Asterisk* indicates a significant pre- to postreduction ($p < 0.01$) in startle amplitude at a given noise burst intensity. Histological reconstructions of the smallest (*left*) and the largest (*right*) electrolytic lesions aimed at the rVNTB/ventrolateral part of the PnO, and the ventrolateral part of the PnC are shown next to the behavioral data. Plates (*A*, bregma −8.00, −8.30, and −9.16 mm; *B*, bregma −8.30, −9.16, and −9.68 mm) used in histological reconstructions of lesions were taken from Paxinos and Watson (1986).

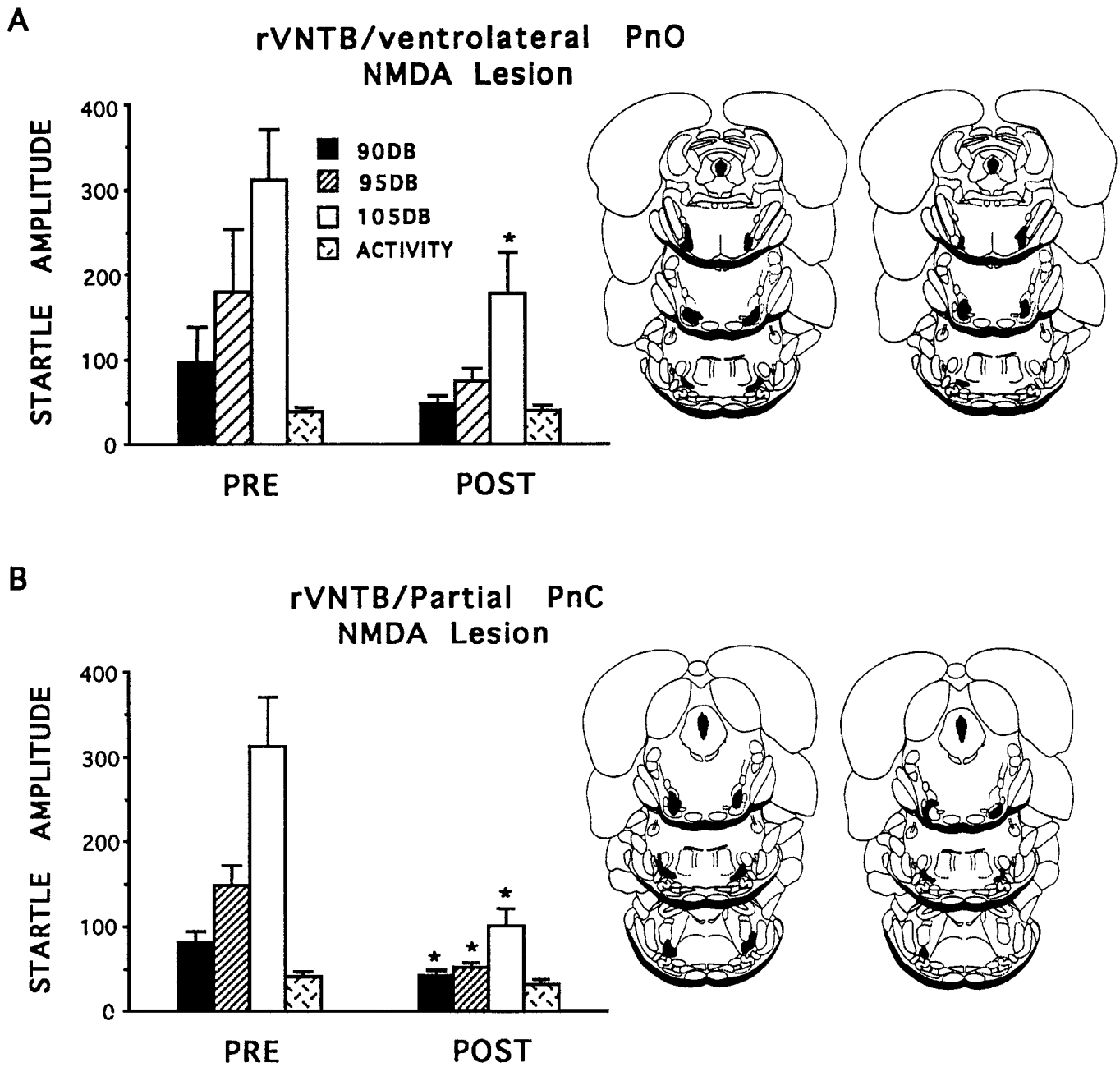

Figure 3. Mean startle amplitude elicited by three different noise burst intensities before and after NMDA lesioning of the the rVNTB/ventrolateral part of the PnO (*A*) or rVNTB/ventrolateral part of the PnO plus partial damage to the anterior ventrolateral part of the PnC (*B*). *Stippled bar* (*Activity*) illustrates animals' mean activity level measured by sampling the cage movement in the absence of startle stimuli. *Asterisk* indicates a significant pre- to postreduction ($p < 0.01$) in startle amplitude at a given noise burst intensity. Histological reconstruction of the smallest (*left*) and the largest (*right*) NMDA lesions in the different areas are shown next to the behavioral data. Plates (*A*, bregma −8.00, −8.30, and −8.80 mm; *B*, bregma −8.30, −8.80, and −9.16 mm) used in histological reconstructions of lesions were taken from Paxinos and Watson (1986).

of the ventrolateral part of the PnC without cell loss in the rVNTB.

The left panel of Figure 3*A* shows that rats with extensive cell loss in the rVNTB and minor cell loss in the posterior aspect of the ventrolateral part of the PnO showed a partial decrease in startle that was statistically significant only at the 105 dB test intensity ($t_{(4)} = 5.38, p < 0.006$). However, this partial reduction in startle probably was not caused by lesions of the rVNTB per se, because some cases ($n = 2$) were found which had no reduction in startle despite lesions that included both the rVNTB and areas rostral to the rVNTB (data not shown). The right panel of Figure 3*A* shows histological reconstructions of the largest and smallest lesions of rVNTB and the posterior aspect of the ventrolateral part of the PnO (area 1). The left panel of Figure 3*B* shows that rats with extensive cell loss in both the rVNTB and the posterior aspect of the ventrolateral part of the PnO and partial cell loss in the anterior aspects of the ventrolateral part of the PnC showed a larger loss of startle that was significant at all three stimulus intensities (90 dB, $t_{(5)} = 4.38, p < 0.007$; 95 dB, $t_{(5)} = 5,97, p < 0.002$; 105 dB, $t_{(5)} = 6.11, p < 0.002$). The right panel of Figure 3*B* shows histological reconstructions of the largest and smallest lesions of this area (area 2). The left panel of Figure 4*A* shows that

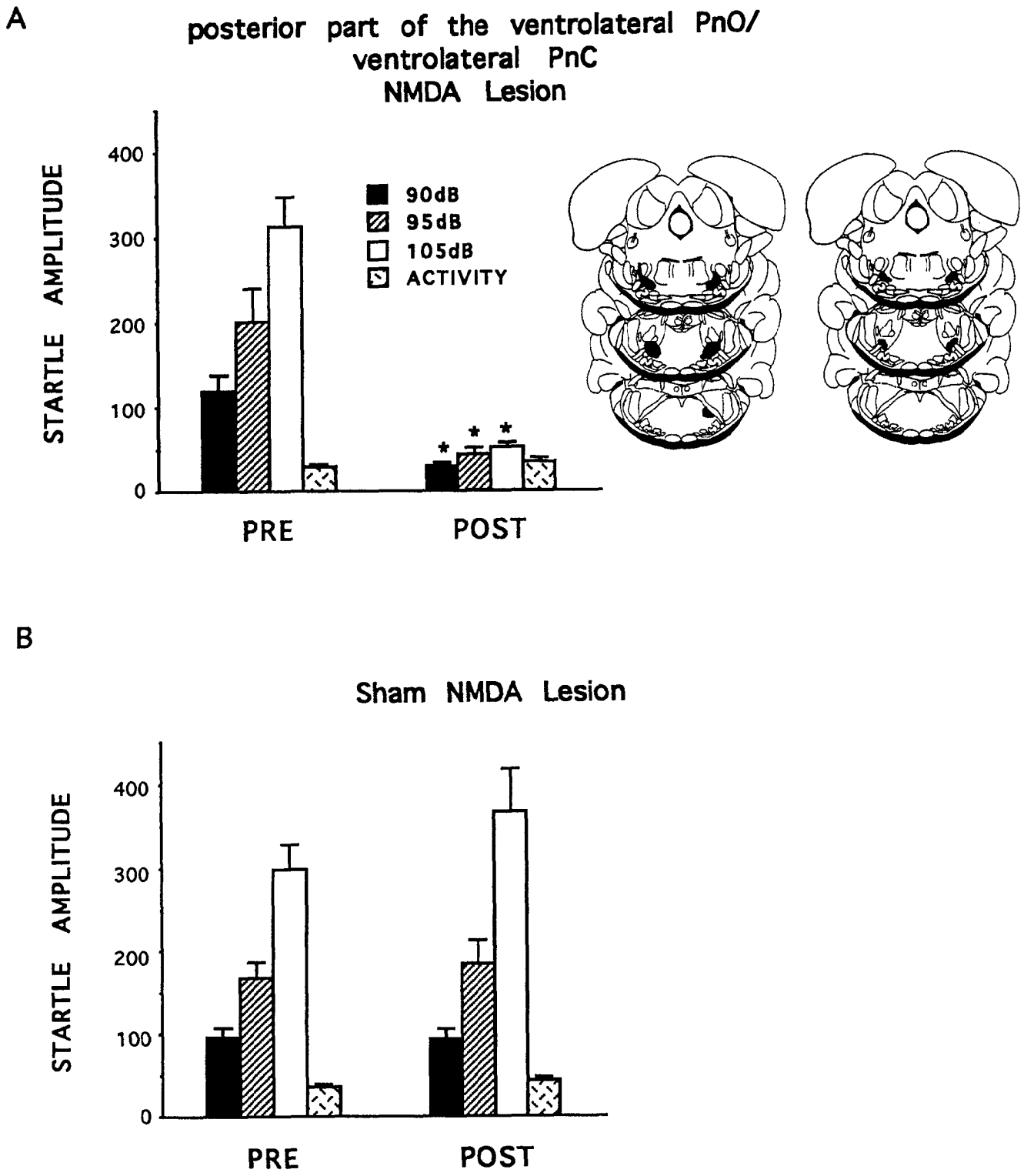

Figure 4. Mean startle amplitude elicited by three different noise burst intensities before and after NMDA lesioning of the posterior part of the ventrolateral part of the PnO and the ventrolateral part of the PnC (*A*) or sham lesioning of rVNTB/ventrolateral part of the PnO and PnC combined (*B*). *Stippled bar* (*Activity*) illustrates animals' mean activity level measured by sampling the cage movement in the absence of startle stimuli. *Asterisk* indicates a significant pre- to postreduction ($p < 0.01$) in startle amplitude at a given noise burst intensity. Histological reconstruction of the smallest (*left*) and the largest (*right*) NMDA lesions in the ventrolateral part of the PnO and the ventrolateral part of the PnC are shown next to the behavioral data. Three plates (bregma −8.80, −9.68, and −10.04 mm) used in histological reconstructions of lesions were taken from Paxinos and Watson (1986).

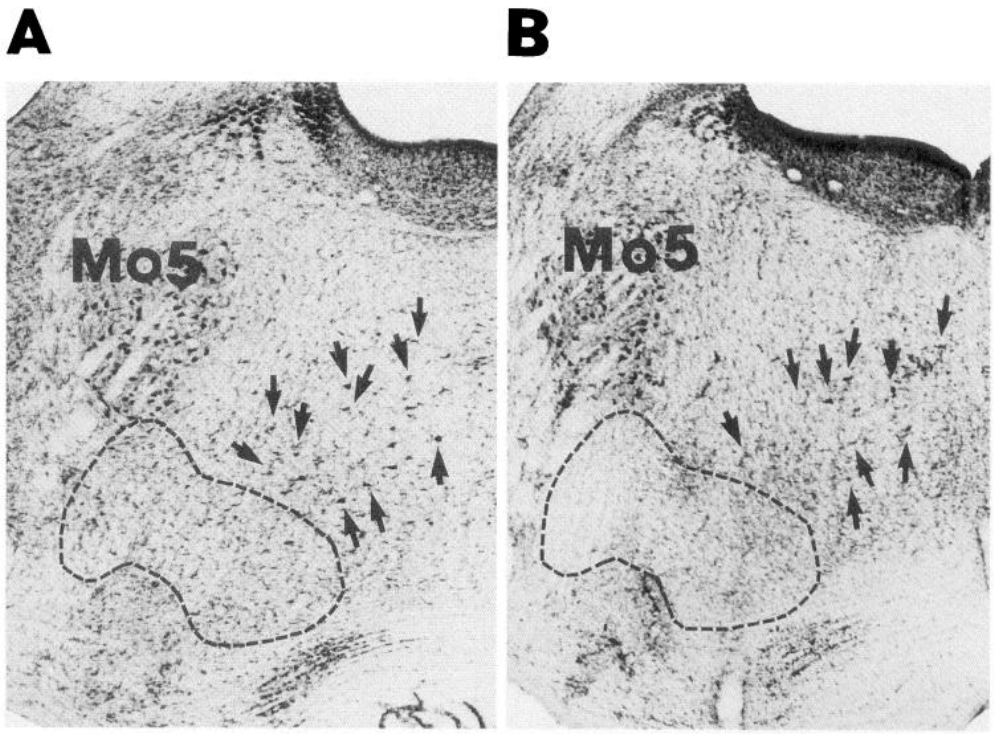

Figure 5. Photomicrographs showing typical sham (*A*) and NMDA (*B*) lesions of the PnC. The encircled area (*broken line*) indicates the location of cell loss. The *arrows* point to more medially located intact giant neurons within the PnC after lesioning.

rats with extensive cell loss in both the posterior aspect of the ventrolateral part of the PnO and the anterior and posterior aspects of the ventrolateral part of the PnC without cell loss in the rVNTB had the greatest reduction in startle. The blockade was significant at all three stimulus intensities (90 dB, $t_{(7)} = 4.50, p < 0.003$; 95 dB, $t_{(7)} = 3.81, p < 0.007$; 105 dB, $t_{(7)} = 6.93, p < 0.000$). In fact, startle in these rats was just barely above the level of cage output sampled in the absence of a startle stimulus (activity sampling; average of 30 units). Thus, if one considers the difference between cage output after a startle stimulus minus cage output during activity sampling as the actual startle amplitude, cell loss in these areas almost completely blocked the startle reflex. The right panel of Figure 4*A* shows histological reconstructions of the largest and smallest lesions of in this area (area 3). In contrast, injections of PB into the same areas (sham lesions) did not affect startle amplitude (Fig. 4*B*).

Photomicrographs shown in Figure 5 illustrate the location and size of a typical NMDA lesion of the PnC area, compared with a sham lesion. Interestingly, NMDA lesions that completely blocked startle typically spared the more medially located giant neurons (*arrows*), which have been implicated in mediating the startle reflex (Koch et al., 1992). Clearly, therefore, additional studies are required to test how cell body-specific lesions restricted only to these medially located giant neurons will affect the acoustic startle response.

Because of the close proximity of the rVNTB, PnO, and PnC, NMDA lesions of any given area always included some cell loss in surrounding areas. Thus, lesions of rVNTB always included some cell loss in the PnO or the PnC, and lesions of the PnC always extended into the PnO. In Figure 6, the behavioral and histological results from these NMDA lesion studies are summarized by grouping the animals based on the extent of the lesion across these three structures. Figure 6*B* shows the mean startle amplitude at the 105 dB test intensity in the sham rats from these various groups and the NMDA lesion groups, ordered in terms of the amount of total cell loss in the ventrolateral parts of the PnO and PnC, extending rostrally to caudally (Fig. 6*A*). When the animals that had damage in area 1, between bregma −8.0 mm and −8.8 mm, according to Paxinos and Watson (1986), were grouped together, they showed a slight attenuation of startle. The animals with cell loss in area 2, between bregma −8.3 mm and −9.16 mm, however, showed a greater attenuation of startle. In the animals with the most extended rostrocaudal lesions, which included the area between bregma −8.8 mm and −10.04 mm (area 3), startle responses were abolished completely.

CRN projections to the PnC

Figure 7 shows the location of the CRNs in the auditory nerve and their trajectory through the ventral acoustic stria and trapezoid body (*A*) and collateral terminals in the PnC (*B*) at a level where NMDA lesions eliminate the acoustic startle reflex (*C*). The plate shown in *C* comes from Paxinos and Watson (1986) at bregma −9.16 mm. This is the closest plate from this atlas that matches the location of the CRN collaterals shown in *B*. However, the actual location of these collaterals is represented more closely by the atlas of Swanson (1992) at bregma −9.25 mm.

Kainic acid lesions of the CRNs

Because of the angular approach and the small diameter of the internal acoustic meatus, lesioning the CRNs proved to be exceedingly difficult. Of the original 40 lesion group animals, 21 did not have any damage to the CRNs and showed no significant change in startle, so their data were excluded. Of the 19 lesioned animals, 10 showed incomplete, mostly unilateral lesions of the CRNs, and their data were analyzed separately. Nine animals showed bilateral lesions of the CRNs. Figure 8*A* shows that bilateral kainic acid lesions of CRNs essentially eliminated the startle response at each of the three test intensities (90 dB, $t_{(8)} = 9.28, p < 0.000$; 95 dB, $t_{(8)} = 9.26, p < 0.000$; 105 dB, $t_{(8)} = 11.09, p < 0.000$). Interestingly, Figure 8*B* shows that the incomplete kainic acid lesions of the CRNs also reduced startle amplitude significantly, although some residual startle clearly was evident.

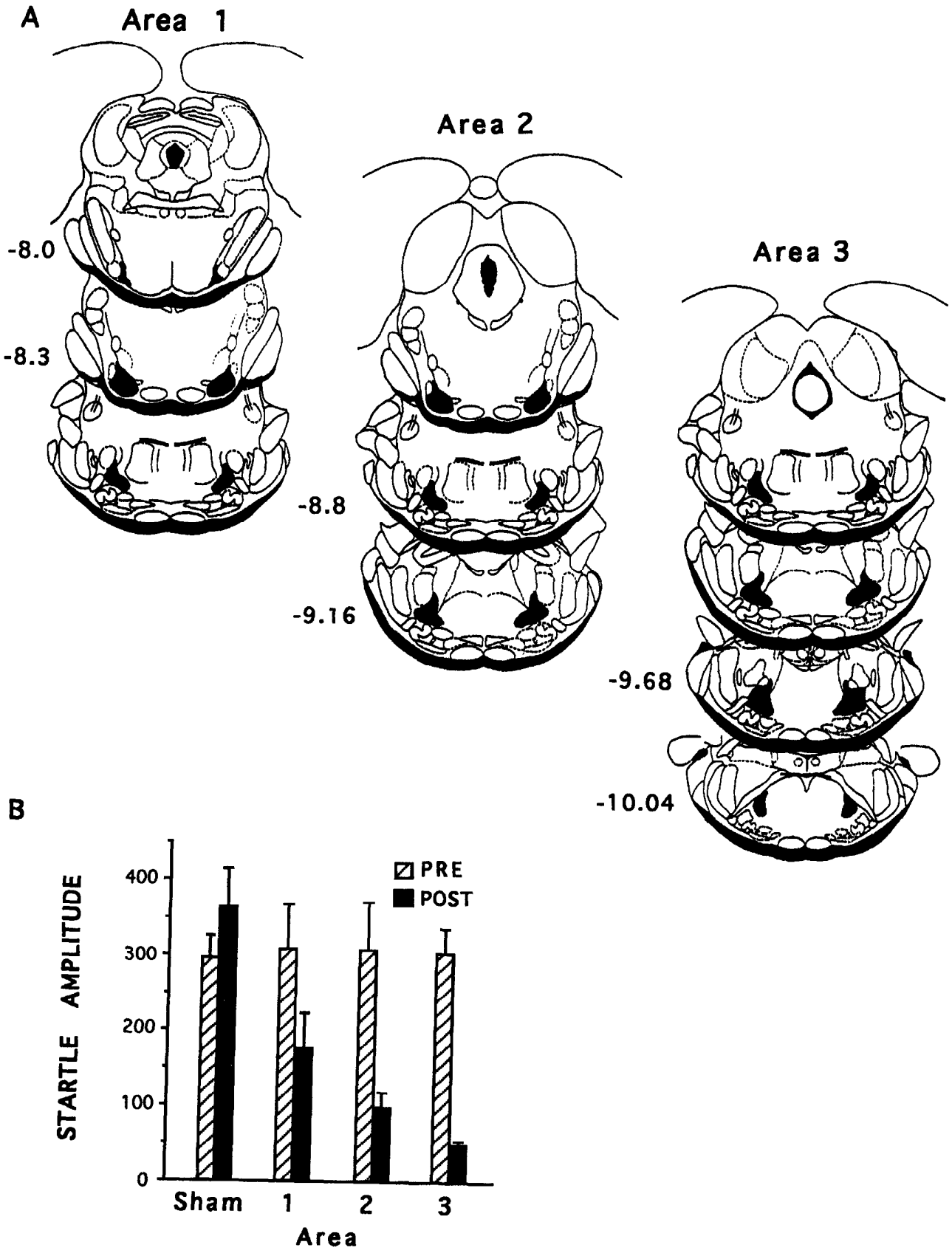

Figure 6. Summary diagram of the mean startle amplitude at the 105 dB test intensity in the sham rats and the NMDA lesion groups ordered in terms of the amount of total cell loss in the ventrolateral parts of the PnO and PnC, extending rostrally to caudally.

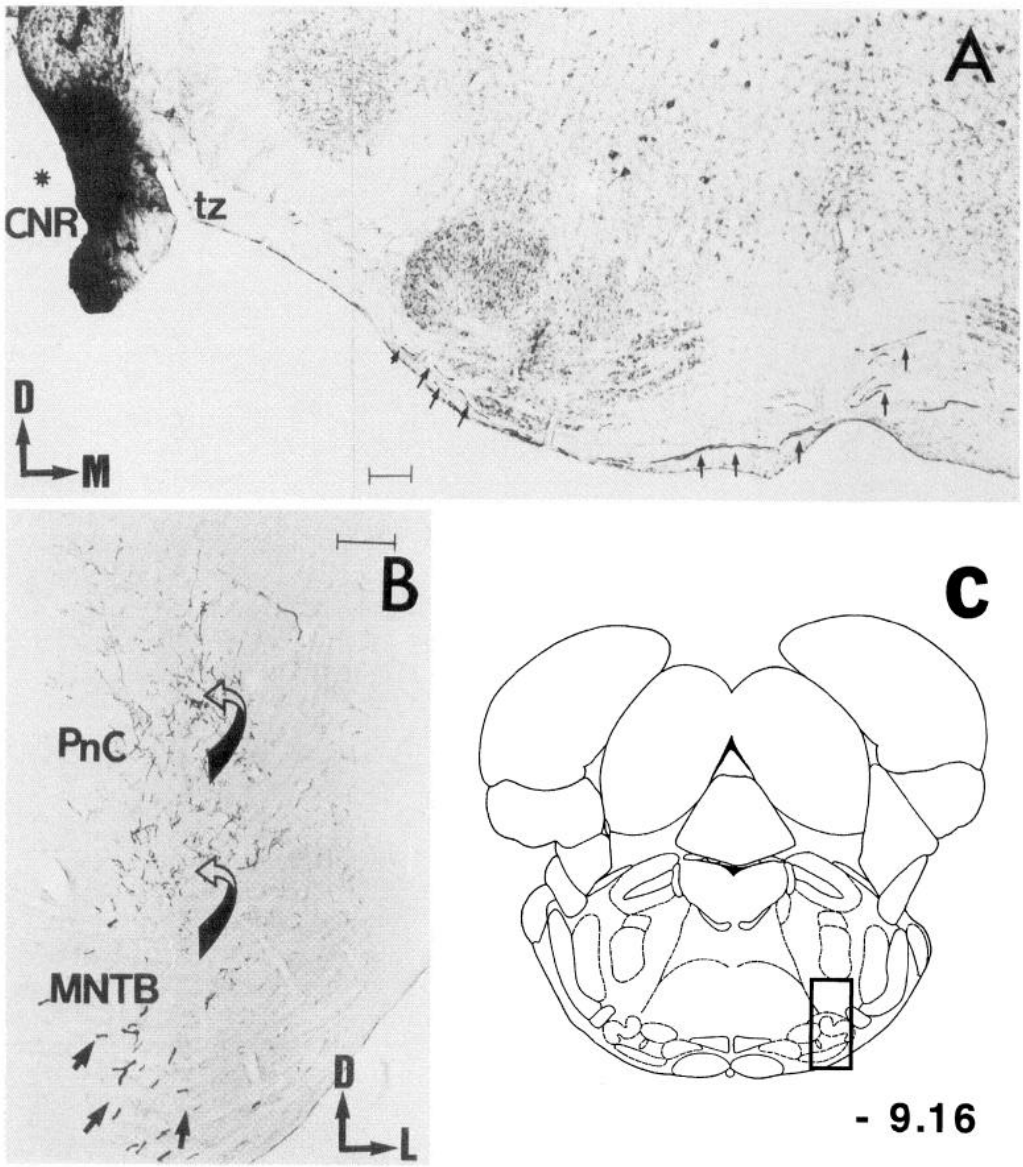

Figure 7. Photomicrographs showing typical BDA injection site for CRNs and the trajectory of their axons through the ventral acoustic stria at the very base of the brain (*A*). *Asterisk* indicates the injection site within the CRNs, and *small arrowheads* indicate axons of the CRNs in the acoustic stria and at the level of the nucleus of the trapezoid body. *B* shows CRN axons (*small arrows*) and collaterals (*large arrows*) terminating in the part of the PnC outlined in the *box* in the coronal section in *C*. Scale bar, 200 μm. The plate shown in *C* comes from Paxinos and Watson (1986) at bregma −9.16 mm. This is the closest plate from the atlas that matches the location of the CRN collaterals shown in *B*. However, the actual location of these collaterals is represented more closely by the atlas of Swanson (1992) at bregma −9.25 mm.

These partial lesions reduced startle amplitude significantly across each of the three test intensities (90 dB, $t_{(9)} = 7.91, p < 0.000$; 95 dB, $t_{(9)} = 6.43, p < 0.000$; 105 dB, $t_{(9)} = 6.00, p < 0.000$). In addition, there were small but significant increases of activity levels after complete as well as incomplete kainic acid lesioning of CRNs. In contrast, Figure 8*C* shows that sham lesions of the CRNs did not change startle amplitude.

Figure 9*A* again shows the location of the CRNs in sham animals, and *C* shows a loss of these cells in rats infused with kainic acid. Figure 9*B* and *D* show the location of CRN axons in the trapezoid body in a sham animal (*B*) and the loss of these axons in animals with kainic acid lesions of CRN cell bodies (*D*).

Compound action potential recording from VCN

The compound action potentials recorded from the VCN after presentation of an auditory stimulus showed two distinct peaks known as the N1 and N2 components. The N1 component is the action potential generated in the auditory nerve itself, whereas the N2 component represents the action potential generated within the cochlear nucleus after a synaptic input from the auditory nerve (Møller, 1983). Measurement of these components was carried out to evaluate whether the auditory nerve was damaged after kainic acid lesioning of the CRNs.

Figure 10*A–C* illustrates representative recordings of the compound action potential generated by an 80 dB, 10 kHz tone pulse from sham-lesioned, kainic acid lesioned, and electrolytic-lesioned animals. These data show that there was no apparent difference in the compound action potential between the sham and kainic acid lesioned animals, which suggests that the auditory nerve had not been damaged by infusion of kainic acid sufficient to destroy CRNs.

Figure 11 summarizes the data for all animals, using the mean amplitudes of the N1 components in the compound action potentials recorded from the VCN. To analyze these data statistically, the mean of the peak N1 amplitudes of the compound action potentials over 15 observations across three intensities (70, 80, and 90 dB) was calculated for each animal. Data from each ear was considered independent data, so that the the number of observations for the statistical analysis was double the number of the subjects for the kainic acid lesion and sham lesion groups (three subjects, 6 data points each). For the electrolytic-lesion

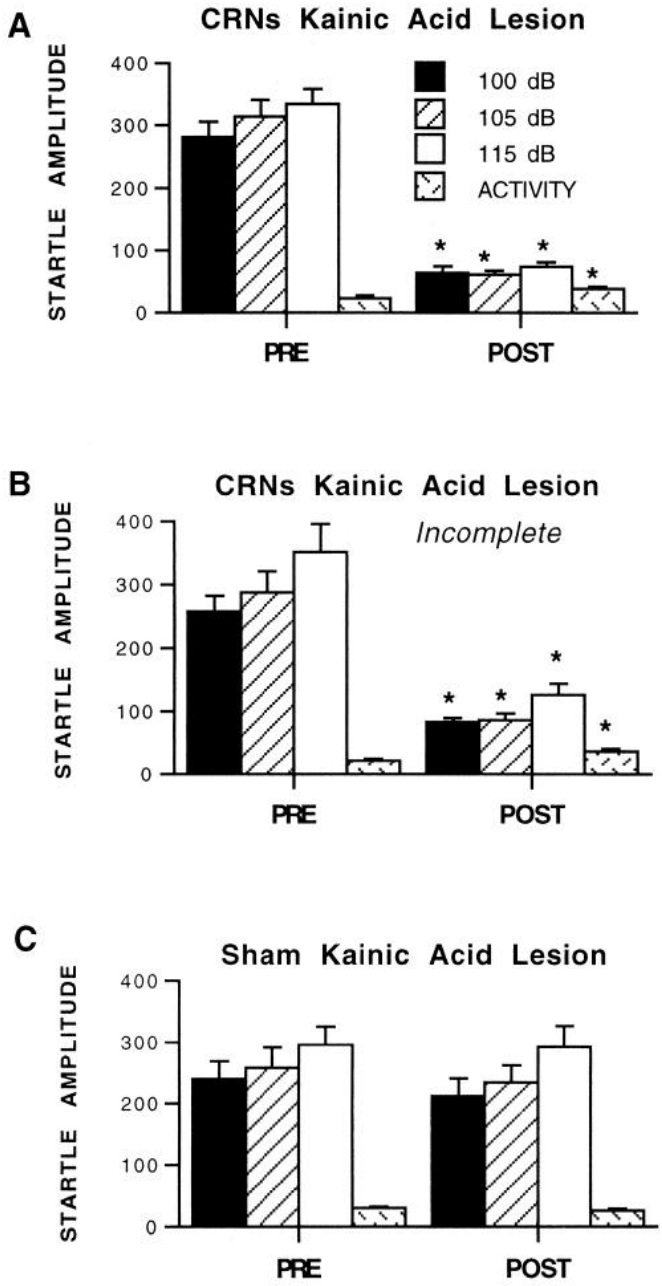

Figure 8. Mean startle amplitude elicited by three different noise burst intensities before and after bilateral kainic acid lesioning of the CRNs (*A*), unilateral–incomplete kainic acid lesioning of the CRNs (*B*), or sham lesioning of the CRNs (*C*). *Stippled bar* (*Activity*) illustrates animals' mean activity level measured by sampling the cage movement in the absence of startle stimuli. *Asterisk* indicates a significant pre- to postreduction ($p < 0.01$) in startle amplitude at a given noise burst intensity after a lesion.

group, because lesions were made unilaterally, the number of observations was same as the number of subjects ($n = 6$).

ANOVA showed a significant lesion effect (kainic acid lesion vs sham lesion vs electrolytic lesion: $F_{(2,30)} = 22.82, p < 0.000$) and an intensity effect ($F_{(2,30)} = 34.08, p < 0.000$). More importantly, there was significant interaction between lesion and intensity ($F_{(4,30)} = 7.79, p < 0.002$). Subsequent post hoc tests showed that there was no significant difference in the peak amplitude of the compound action potentials between the kainic acid-lesioned animals and the sham-lesioned animals. However, the peak amplitude of the compound action potentials in the electrolytic-

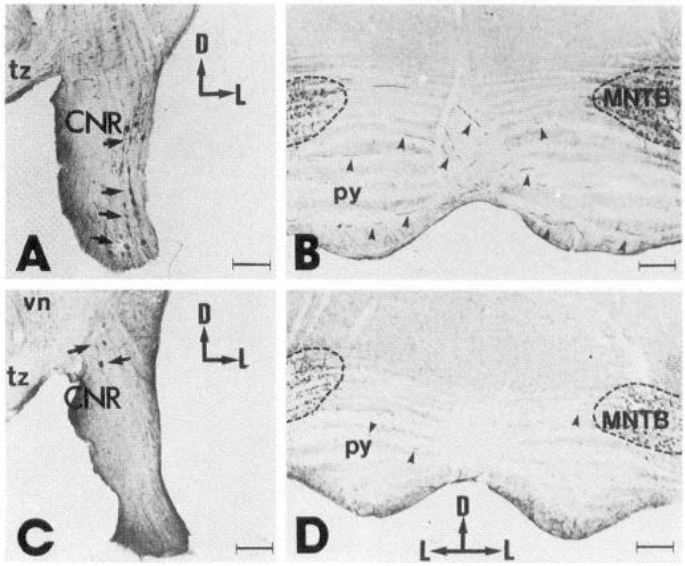

Figure 9. CRNs after sham lesioning (*A*) or kainic acid lesioning (*C*). *Left panels* show CRN axons traveling through the trapezoid body after sham lesioning (*B*) or kainic acid lesioning of the CRNs (*D*). *Small arrowheads* indicate the location of the axons stained with Calbindin D-28K. After kainic acid lesioning, axons show severe degeneration, whereas no visible damage was observed after sham lesioning.

lesioned animals was significantly smaller than those of the sham-lesioned animals at each of the three test intensities (70 dB, $F_{(1,30)} = 6.63, p < 0.015$; 80 dB, $F_{(1,30)} = 22.61, p < 0.000$; 90 dB, $F_{(1,30)} = 49.41, p < 0.000$). Comparisons between the kainic acid-lesioned animals and the electrolytic-lesioned animals also showed significant differences at 70 dB ($F_{(1,30)} = 5.37, p < 0.027$), 80 dB ($F_{(1,30)} = 20.62, p < 0.000$), and 90 dB ($F_{(1,30)} = 55.33, p < 0.000$), indicating that the auditory nerve was functionally intact after the kainic acid lesioning but not after the electrolytic lesioning of the CRNs.

DISCUSSION

Davis et al. (1982) proposed a primary acoustic startle circuit in rats that consisted of the auditory nerve, PVCN, an area ventral and medial to the VLL, the PnC, and spinal motoneurons. The present study evaluated the role of the VLL, the VLTg, the rVNTB (previously known as the periolivary nucleus), and the PnC in mediating the acoustic startle reflex using more recently developed fiber-sparing, cell-specific chemical lesions. Special emphasis also was placed on evaluating the role of neurons embedded in the auditory nerve (CRNs) that have direct projections to the PnC. Chemical lesions of CRNs or ventrolateral parts of the PnC eliminated startle, whereas lesions of the VLL, VLTg, or rVNTB did not. Although the role of the PVCN, originally suggested as critical for startle, is still unclear, the primary acoustic startle pathway in rats may consist of only three synapses onto (1) CRNs, (2) neurons in ventrolateral parts of the PnC, and (3) spinal motoneurons (Fig. 12).

CRNs

In the rat, CRNs are activated by collaterals from the auditory nerve even before these auditory nerve fibers reach the cochlear nucleus complex (Harrison and Warr, 1962; Osen et al., 1991). However, CRNs send thick axons and axon collaterals to brainstem areas not known traditionally as part of the central auditory system (López et al., 1993a). The neuroanatomical characteristics

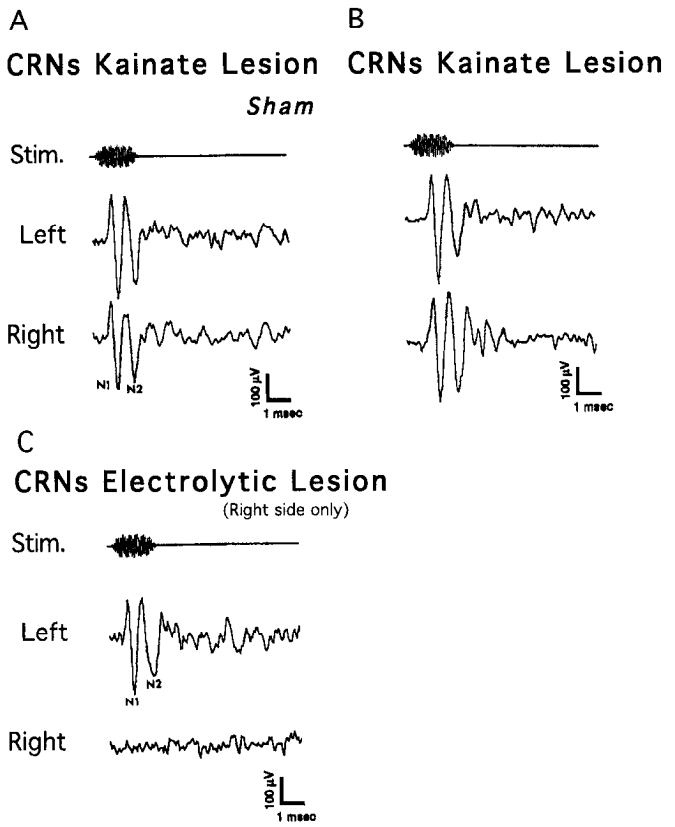

Figure 10. Individual compound action potential recording (N1 wave–auditory nerve response; N2 wave–cochlear nucleus response) from a sham-lesioned, kainic acid-lesioned, and electrolytic-lesioned animal in response to an 80 dB, 10 kHz tone burst.

of their projections suggested the involvement of CRNs in the acoustic startle reflex (López et al., 1993b; Lingenhöhl and Friauf, 1994). Their axons run in the ventral acoustic stria (Fig. 6*A*), lesions of which abolished the acoustic startle reflex (Davis et al., 1982). Axon collaterals of CRNs synapse mainly in ventrolateral parts of the PnC (López et al., 1993b), known to be critical in acoustic startle.

CRNs have thick soma diameters, about 35 μm, and have well-myelinated large axons that average 3.7 μm in diameter (Harrison and Irving, 1965; Merchán et al., 1988). This suggests fast-conducting axonal properties, which would be critical for neurons mediating a short-latency reflex, such as acoustic startle (Yeomans et al., 1989).

Bilateral kainic acid lesions of CRNs abolished the acoustic startle reflex completely. This blockade did not appear to result from damage of the auditory nerves per se, because lesioned animals showed normal orienting behaviors (data not shown) and normal compound action potentials recorded from the cochlear nucleus. These data provide the first direct evidence that CRNs may contain the first synaptic relay in the acoustic startle reflex.

In our previous studies (Davis et al., 1982), electrolytic lesions of the PVCN abolished startle, whereas stimulation of the PVCN elicited startle-like responses. Although the role of the PVCN should be reevaluated carefully (see below), given the large lesion size and nonselective nature of electrical stimulation, we now believe these original observations result from lesions or stimulation of CRN axons.

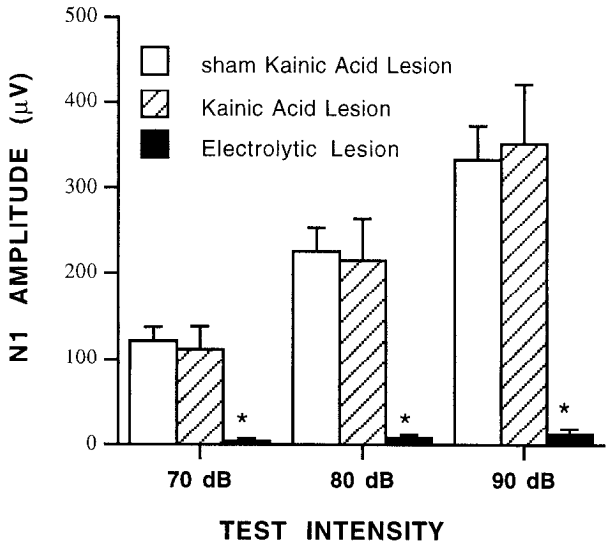

Figure 11. Summary data illustrating mean amplitudes of the auditory nerve response (N1 component of the compound action potential) in sham-lesioned, kainic acid-lesioned, and electrolytic-lesioned animals at three different intensities.

VLL and VLTg

Because electrolytic lesions of the area medial and ventral to the VLL abolished startle, and electrical stimulation of this area elicited startle-like responses, this area was included as the second synapse in startle reflex pathway (Davis et al., 1982). Subsequently, it was deemed important in acoustic head startle (Pellet, 1990) and whole body startle (Frankland et al., 1995).

In the present study, small, discrete electrolytic lesions of the VLL and adjacent areas such as VLTg and rVNTB did not block startle. However, whenever these lesions invaded at least the anterior part of the ventrolateral part of the PnC, they significantly reduced startle amplitude (e.g., Fig. 2*B*), suggesting that only the PnC is necessary in mediating acoustic startle. Considering the anatomical proximity (less than 1 mm separation) between the ventrolateral part of the PnC and the areas adjacent to the VLL, we now believe that our original lesion and stimulation data resulted from damage to, or stimulation of, anterior regions of the ventrolateral part of the PnC. Alternatively, electrolytic lesions of this area would have destroyed CRN axons of passage (López et al., 1993) and eliminated startle via subsequent degeneration of CRNs. Preliminary results show that unilateral electrolytic lesions of the VLTg and anterior ventrolateral part of the PnC, even smaller than those of our original study, induced substantial degeneration of CRNs axons and cell bodies in the contralateral auditory nerve ($n = 2$) (Y. Lee, D. López, and M. Davis, unpublished observations). More recently, Frankland et al. (1995) have suggested that a synapse exists in the VLTg that is involved in the acoustic startle reflex based on electrical stimulation of the anterior ventral cochlear nucleus using currents greater than 1,500 μA in anesthetized rats. We have not found that lesions of the anteroventral cochlear nucleus block startle (E. Meloni, Y. Lee, and M. Davis, unpublished observations). Hence, such high-stimulation currents may have spread to other brain areas to elicit motor movements that look like startle but may involve pathways other than those normally used by physiological stimuli.

rVNTB

Rats with extensive cell loss in the rVNTB and minor cell loss in the posterior aspect of the ventrolateral part of the PnO showed

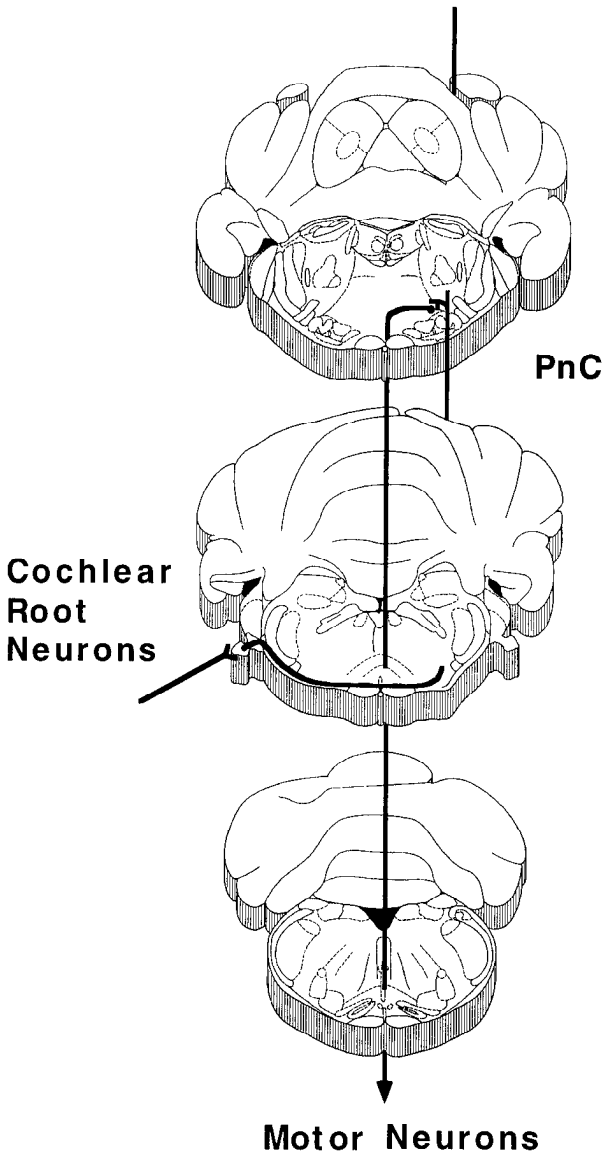

Figure 12. Diagram illustrating a primary acoustic startle circuit consisting of the CRNs, the ventrolateral part of the PnC, and axons projecting to motoneurons in the spinal cord.

a partial decrease in startle that was statistically significant only at the 105 dB test intensity. However, this partial reduction in startle probably was not caused by lesions of the rVNTB per se, because electrolytic lesions of the VLTg and rVNTB alone did not affect startle at any intensity and two cases with NMDA lesions were found that had no reduction in startle despite cell loss in both the rVNTB and areas rostral to the rVNTB.

PnC

NMDA lesions of the ventrolateral part of the PnC blocked startle completely, further supporting the essential role of the PnC in the acoustic startle response (Szabo and Hazafi, 1965; Hammond, 1973; Rossignol, 1973; Groves et al., 1974; Leitner et al., 1980; Davis et al., 1982; Gokin and Karpukhina, 1985; Cassella and Davis, 1986; Wu et al., 1988; Yeomans et al., 1989; Pellet, 1990; Koch et al., 1992; Lingenhöhl and Friauf, 1992; Yeomans et al., 1993; Lingenhöhl and Friauf, 1994; Frankland et al., 1995). The critical parts of the PnC where chemical lesions eliminated startle were the areas dorsal to the superior olivary complex and ventral to the motor trigeminal nucleus (Mo5). This area also is critical for the pinna component of the startle reflex. It has direct projections to the ventral medial division of the facial motor nucleus, which contains the motoneurons that move the pinna backwards, and lesions of this area block the acoustically elicited pinna response completely (Meloni and Davis, 1992). This is the area where CRN collaterals terminate (Fig. 10*B*) (López et al., 1993) and the part of the PnC identified as a critical synapse in acoustic startle using electrical stimulation techniques (Yeomans et al., 1993; Frankland et al., 1995).

Infusion of excitatory amino acid antagonists into the ventrolateral part of the PnC almost totally blocked startle at very low doses (Krase et al., 1993; Miserendino and Davis, 1993). Earlier, Spiera and Davis (1988) reported that excitatory amino acid antagonists infused into the vicinity of the VLL reduced startle amplitude markedly. However, the doses infused into this area were 50–60 times higher than those required to produce a comparable depression of startle after infusion into the PnC (Miserendino and Davis, 1993). Hence, depression of startle after infusion into the vicinity of the VLL probably resulted from drug diffusion into the ventrolateral part of the PnC. In fact, exploratory studies showed that infusion of CNQX into the VLL did not affect startle (Y. Lee and M. Davis, unpublished observations) at a dose that did after infusion into the PnC (Miserendino and Davis, 1993). These data further support the idea that the VLL and surrounding areas are not involved in acoustic startle, whereas the ventrolateral part of the PnC is. PnC neurons project to spinal motoneurons (Grillner and Lund, 1968; Grillner et al., 1971; Peterson, 1979; Peterson et al., 1979; Tohyama et al., 1979; Lingenhöhl and Friauf, 1994), making both mono- and polysynaptic connections.

Alternative, modulatory pathways

Others have reported startle reflexes in rats with latencies longer than 8 msec. Fox (1979) recorded muscle activation in the neck that had an 11 msec latency, and Szabo (1965) and Prosser and Hunter (1936) reported latencies in the hindlegs as long as 15–25 msec. Hence, alternative pathway(s) that include more than three synapses may exist that eventually converge at some point with the trisynaptic pathway outlined above.

One possible alternative pathway might involve the VCN, superior olive, dorsal nucleus of the lateral lemniscus, the PnC, and spinal motoneurons (Davis et al., 1982). Another might include the dorsal cochlear nucleus (DCN), the VLTg, the PnC, and spinal motoneurons. The VCN and the DCN clearly respond to auditory information and send heavy projections to the PnC directly and indirectly (Kandler and Herbert, 1991). Although our lesion study concluded otherwise, involvement of the VLTg in the startle reflex has been suggested by Frankland et al. (1995). Although Lingenhöhl and Friauf (1994) ruled out the VLTg because acoustically driven neurons showed long response latencies, it still might be involved in a longer-latency response.

Another possibility would be that the short- and long-latency components of startle reflect activation of different neurotransmitters involved in startle. Boulis et al. (1990) found that intrathecal infusion of CNQX preferentially blocked the early EMG component of startle measured in the hindlimb (8 msec latency), whereas infusion of an NMDA receptor antagonist preferentially blocked the late component (15 msec latency). As discussed at length in Boulis et al. (1990), short-latency EMG components of startle might reflect rapidly occurring excitatory postsymatic po-

tential mediated by non-NMDA receptors, whereas the longer-latency components might reflect slower excitatory postsynaptic potentials mediated by NMDA receptors. If so, then more complex neural pathways would not be required to account for these longer-latency startle responses.

CONCLUSION

A primary acoustic startle circuit

The present series of experiments provides the first clear evidence suggesting that CRNs form the first synapse in a primary acoustic startle circuit. The second synapse likely occurs not in the VLTg area but at the level of the ventrolateral part of the PnC. The elimination of a second synapse in the VLTg area originally was proposed based on lesion studies (Lee and Davis, 1992) and later supported by Lingenhöhl and Friauf (1994). The present electrolytic and chemical lesion studies further confirm this speculation and suggest that a primary acoustic startle circuit consists of CRNs, the ventrolateral part of the PnC, and spinal motoneurons (Fig. 12).

REFERENCES

Adams LM, Geyer MA (1981) Effects of 6-hydroxydopamine lesions of locus coeruleus on startle in rats. Psychopharmacology 73:394–398.

Boulis NM, Kehne JH, Miserendino MJD, Davis M (1990) Differential blockade of early and late components of acoustic startle following intrathecal infusion of 6-cyano-7-nitroquinoxaline-2,3-dione (CNQX) or D,L-2-amino-5-phosphonovaleric acid (AP-5). Brain Res 520:240–246.

Bradley MM, Lang PJ, Cuthbert BN (1993) Emotion, novelty, and the startle reflex: habituation in humans. Behav Neurosci 107:970–980.

Braff DL, Stone C, Callaway E, Geyer M, Glick I, Bali L (1978) Prestimulus effects on human startle reflex in normals and schizophrenics. Psychophysiology 15:339–343.

Braff DL, Grillon C, Geyer MA (1992) Gating and habituation of the startle reflex in schizophrenic patients. Arch Gen Psychiatry 49:206–215.

Brown JS, Kalish HI, Farber IE (1951) Conditional fear as revealed by magnitude of startle response to an auditory stimulus. J Exp Psychol 41:317–328.

Cassella JV, Davis M (1986) Neural structures mediating acoustic and tactile startle reflexes and the acoustically-elicited pinna response in rats: electrolytic and ibotenic acid studies. Soc Neurosci Abstr 12:1273.

Cook III EW, Davis TL, Hawk LW, Spence EL, Gautier CH (1992) Fearfulness and startle potentiation during aversive stimulation. Psychophysiology 663–645.

Cory RN, Ison JR (1979) Persistent effect of noise on the acoustic startle reflex in the rat. Anim Learn Behav 7:367–371.

Davis M (1970) Effects of interstimulus length and variability on habituation of the acoustic startle reflex in the rat. J Comp Physiol Psychol 72:177–192.

Davis M (1974) Sensitization of the rat startle response by noise. J Comp Physiol Psychol 87:571–581.

Davis M (1980) Neurochemical modulation of sensory-motor reactivity: acoustic and tactile startle reflexes. Neurosci Biobehav Rev 4:241–263.

Davis M (1989) Sensitization of the acoustic startle reflex by footshock. Behav Neurosci 103:495–503.

Davis M, Astrachan DI (1978) Conditioned fear and startle magnitude: effects of different footshock or backshock intensities used in training. J Exp Psychol Anim Behav Process 4:95–103.

Davis M, Heninger GR (1972) Comparison of response plasticity between the eyeblink and vertex potential in humans. Electroencephalogr Clin Neurophysiol 33:283–293.

Davis M, Gendelman DS, Tischler MD, Gendelman PM (1982) A primary acoustic startle circuit: lesion and stimulation studies. J Neurosci 6:791–805.

Davis M, Falls WA, Campeau S, Kim M (1993) Fear-potentiated startle: a neural and pharmacological analysis. Behav Brain Res 58:175–198.

Fillon DL, Dawson ME, Schell AM (1993) Modification of the acoustic startle-reflex eyeblink: a tool for investigating early and later attentional processes. Biol Psychol 35:185–200.

Fox JE (1979) Habituation and prestimulus inhibition of the auditory startle reflex in decerebrate rats. Physiol Behav 23:291–297.

Frankland PW, Scott BW, Yeomans JS (1995) Axons and synapses mediating electrically evoked startle: collision tests and latency analysis. Brain Res 670:97–111.

Geyer MA, Braff DL (1987) Startle habituation and sensorimotor gating in schizophrenia and related animal models. Schizophr Bull 13:643–668.

Gokin AP, Karpukhina MV (1985) A study of reticular structures in cat brain involved in startle reflexes to somatic stimuli of different modalities. Neurophysiology (USSR) 17:380–390.

Graham F (1975) The more or less startling effects of weak prestimulus. Psychophysiology 12:238–248.

Grillner S, Lund S (1968) The origin of a descending pathway with monosynaptic action on flexor motoneurons. Acta Physiol Scand 74:274–284.

Grillner S, Honogo T, Lund S (1971) Convergent effects on alpha motoneurons from the vestibulospinal tract and a pathway descending the medial longitudinal fasciculus. Exp Brain Res 12:457–479.

Grillon C, Ameli R, Woods SW, Merikangas K, Davis M (1991) Fear-potentiated startle in humans: effects of anticipatory anxiety on the acoustic blink reflex. Psychophysiology 28:588–595.

Groves PM, Thompson RF (1970) Habituation: a dual process theory. Psychol Rev 77:419–450.

Groves PM, Wilson CJ, Boyle RD (1974) Brain stem pathways, cortical modulation and habituation of the acoustic startle response. Behav Biol 10:391–418.

Hammond GR (1973) Lesions of pontine and medullary reticular formation and prestimulus inhibition of the acoustic startle in rats. Physiol Behav 10:239–243.

Harrison JM, Irving R (1965) The anterior ventral cochlear nucleus. J Comp Neurol 124:15–42.

Harrison JM, Warr WB (1962) A study of the cochlear nucleus and ascending auditory pathways of the medulla. J Comp Neurol 119:341–379.

Hoffman HS, Ison JR (1980) Reflex modulation in the domain of startle. I. Some empirical findings and their implications for how the nervous system processes sensory input. Psychol Rev 87:175–189.

Hoffman HS, Stitt C (1969) Behavioral factors in habituation of acoustic startle reactions. J Comp Physiol Psychol 68:276–279.

Hoffman HS, Marsh RR, Stein N (1969) Persistence of background acoustic stimulation in controlling startle. J Comp Physiol Psychol 68:280–283.

Ison JR (1982) Temporal acuity in auditory function in the rat: reflex inhibition by brief gaps in noise. J Comp Physiol Psychol 96:945–954.

Ison JR, Hammond G (1971) Modification of the startle reflex in the rat by changes in the auditory and visual environment. J Comp Physiol Psychol 75:435–452.

Ison JR, McAdam DW, Hammond GR (1973) Latency and amplitude changes in the acoustic startle reflex of the rat produced by variation in auditory prestimulation. Physiol Behav 10:1035–1039.

Jordan WP (1989) Mesencephalic reticular formation lesions made after habituation training abolish long-term habituation of the acoustic startle response in rats. Behav Neurosci 103:805–815.

Kandler K, Herbert H (1991) Auditory projections from the cochlear nucleus to pontine and mesencephalic reticular nuclei in the rat. Brain Res 562:230–242.

Klüver H, Barrera A (1953) A method for the combined staining of cells and fibres of the nervous system. J Neuropathol Exp Neurol 12:400.

Koch M, Lingenhöhl K, Pilz PKD (1992) Loss of the acoustic startle response following neurotoxic lesions of the caudal pontine reticular formation: possible role of giant neurons. Neuroscience 49:617–625.

Koch M, Kungel M, Herbert H (1993) Cholinergic neurons in the pedunculopontine tegmental nucleus are involved in the mediation of prepulse inhibition of the acoustic startle response in the rat. Exp Brain Res 97:71–82.

Kokkinidis L (1986) Sensitization to amphetamine and tolerance to cocaine and phencyclidine stimulation in mice. Pharmacol Biochem Behav 25:1175–1180.

Korn JH, Moyer KE (1965) The effects of pre-shock and handling on the startle response in the rat. Psychon Sci 3:409–410.

Krase W, Koch M, Schnitzler HU (1993) Glutamate antagonists in the reticular formation reduce the acoustic startle reflex. NeuroReport 4:13–16.

Krase W, Koch M, Schnitzler HU (1994) Substance P is involved in the sensitization of the acoustic startle response by footshock in rats. Behav Brain Res 63:81–88.

Landis C, Hunt W (1939) The startle paradigm. New York: Farrar and Rinehart.

Lang PJ, Bradley MM, Cuthbert BN (1990) Emotion, attention, and the startle reflex. Psychol Rev 97:377–395.

Leaton RN (1976) Long-term retention of the habituation of lick suppression and startle response produced by a single auditory stimulus. J Exp Psychol Anim Behav Process 3:248–259.

Leaton RN, Supple WF (1986) Cerebellar vermis: essential for long-term habituation of the acoustic startle response. Science 232:513–515.

Lee Y, Davis M (1992) A primary acoustic startle circuit: lesion and anatomical tracing studies. Soc Neurosci Abstr 18:1563.

Leitner DS, Powers AS, Hoffman HS (1980) The neural substrate of the startle response. Physiol Behav 25:291–297.

Lingenhöhl K, Friauf E (1992) Giant neurons in the caudal pontine reticular formation receive short latency acoustic input: an intracellular recording and HRP study in the rat. J Comp Neurol 325:473–492.

Lingenhöhl K, Friauf E (1994) Giant neurons in the rat reticular formation: a sensorimotor interface in the elementary acoustic startle circuit? J Neurosci 14:1176–1194.

Lipp OV, Sheridan J, Siddle DA (1994) Human blink startle during aversive and nonaversive Pavlovian conditioning. J Exp Psychol Anim Behav Process 20:380–389.

López DE, Merchán MA, Bajo VM, Saldana E (1993a) The cochlear root neurons in the rat, mouse and gerbil. In: The mammalian cochlear nuclei: organization and function (Merchán MA, ed), pp 291–301. New York: Plenum.

López DE, Warr WB, Sinex DG (1993b) The cochlear root neurons: first sentinels of the auditory pathway. Sixteenth ARO meeting Abstract 471.

Mansbach RS, Geyer MA (1991) Parametric determinants in prestimulus modification of acoustic startle: interaction with ketamine. Psychopharmacology 105:162–168.

Meloni EG, Davis M (1992) Anatomical connections mediating the pinna component of the acoustic startle reflex in the rat. Soc Neurosci Abstr 18:1547.

Merchán MA, Collía F, López DE, Saldaña E (1988) Morphology of cochlear root neurons in the rat. J Neurocytol 17:711–725.

Miserendino MJD, Davis M (1993) NMDA and non-NMDA antagonists infused into the nucleus reticularis pontis caudalis depress the acoustic startle reflex. Brain Res 623:215–222.

Mller AR (1983) On the origin of the compound action potentials (N1, N2) of the cochlear of the rat. Exp Neurol 80:633–644.

Ornitz EM, Guthrie D, Kaplan AR, Lane SJ, Norman RJ (1986) Maturation of startle modulation. Psychophysiology 23:624–634.

Osen KK, López DE, Slyngstad TA, Ottersen OP, Storm-Mathisen J (1991) GABA-like and glycine-like immunoreactivities of the cochlear root nucleus in rat. J Neurocytol 20:17–25.

Parham K, Willott JF (1990) Effects of inferior colliculus lesions on the acoustic startle response. Behav Neurosci 104:831–840.

Paxinos G, Watson C (1986) The rat brain in stereotaxic coordinates. New York: Academic.

Pellet J (1990) Neural organization in the brainstem circuit mediating the primary acoustic head startle: an electrophysiological study in the rat. Physiol Behav 48:1–10.

Peterson BW (1979) Reticulospinal projection to spinal motor nuclei. Annu Rev Physiol 41:127–140.

Peterson BW, Pitts NG, Fukushima K (1979) Reticulospinal connections with limb and axial motoneurons. Exp Brain Res 36:1–20.

Prosser CL, Hunter WS (1936) The extinction of startle responses and spinal reflexes in the white rat. Am J Physiol 117:609–618.

Rossignol S (1973) Auditory influence on motor systems. Unpublished dissertation, McGill University.

Russo JM, Ison JR (1979) Sensitization of the rat's acoustic startle response by repetition of a photic stimulus. Physiol Psychol 7:102–106.

Spiera RF, Davis M (1988) Excitatory amino acid antagonists depress acoustic startle after infusion into the ventral nucleus of the lateral lemniscus or paralemniscal zone. Brain Res 445:130–136.

Swanson LW (1992) Brain maps: structure of the rat brain. New York: Elsevier.

Swerdlow NR, Geyer MA, Vale WW, Koob GF (1986) Corticotropin-releasing factor potentiates acoustic startle in rats: blockade by chlordiazepoxide. Psychopharmacology 88:147–152.

Swerdlow NR, Caine SB, Braff DL, Geyer MA (1992) The neural substrates of sensorimotor gating of the startle reflex: a review of recent findings and their implications. J Psychopharmacol 6:176–190.

Szabo I (1965) Analysis of the muscular action potentials accompanying the acoustic startle reaction. Acta Physiol Acad Sci Hung 27:167–178.

Szabo I, Hazafi K (1965) Elicitability of the acoustic startle reaction after brain stem lesions. Acta Physiol Acad Sci Hung 27:155–165.

Tohyama M, Sakai K, Salvert D, Touret M, Jouvet M (1979) Spinal projections from the lower brainstem in the cat as demonstrated by the horseradish technique. I. Origins of the reticulospinal tracts and their funicular trajectories. Brain Res 173:383–403.

Wu MF, Suzuki SS, Siegel JM (1988) Anatomical distribution and response patterns of reticular neurons in relation to acoustic startle. Brain Res 457:399–406.

Yeomans JS, Cochrane KA (1993) Collision-like interactions between acoustic and electrical signals that produce startle reflexes in reticular formation sites. Brain Res 320–328.

Yeomans JS, Rosen JB, Barbeau J, Davis M (1989) Double-pulse stimulation of startle-like responses in rats: refractory periods and temporal summation. Brain Res 486:147–158.

Yeomans JS, Hempek CME, Chapman CA (1993) Axons and synapses mediating startle-like responses evoked by electrical stimulation of the reticular formation in rats: symmetric and asymmetric collision effects. Brain Res 617:309–319.